38

Low-Loss and No-Loss Spectra and Images

CHAPTER PREVIEW

The term 'energy loss' implies that we are interested only in inelastic interactions, but the spectrum will also contain electrons which have not lost any discernible energy, so we need to consider elastic scattering as well. In this chapter, we'll focus on the low-energy portion of the EEL spectrum which comprises

- The zero-loss peak, which primarily contains elastic, forward-scattered electrons, but also includes electrons that have suffered small energy losses. Forming images and DPs with the zero-loss electrons offers tremendous advantages over unfiltered images, particularly from thicker specimens.
- The low-loss region up to an (arbitrary) energy loss of $\sim$ 50 eV contains electrons which have interacted with the weakly bound, outer-shell electrons of the atoms. Thus, this part of the spectrum reflects the dielectric response of the specimen to high-energy electrons. We can also form images from these low-loss electrons that reveal information about the electronic structure and other characteristics of the specimen.

The energy-loss spectrum is more useful than an X-ray spectrum which only contains elemental information. However, this kind of spectrum is also far more complex. To understand its content you need a greater understanding of the physics of beam-specimen interactions, so we'll give you some hints about where to get the necessary education.

38.1 A FEW BASIC CONCEPTS

Back in Chapters 2–4, we described the difference between elastic and inelastic beam-specimen interactions and introduced the ideas of scattering cross sections and the associated mean free path. Remember, the cross section is a measure of the probability of a specific scattering event occurring and the mean free path is the average distance between particular interactions. It might be a good idea to re-read about those ideas before starting on this chapter. Briefly, you should recall that elastic scattering is an electron-nucleus interaction; the word elastic implies that there is no energy loss, although a change in direction, and hence in momentum, usually occurs. Elastic scattering occurs mainly as Bragg diffraction in crystalline specimens. Inelastic scattering is primarily an electron-electron interaction and entails both a loss of energy and a change of momentum.

We have to be concerned with both the amount of energy lost and the direction of the electrons after they've come through the specimen.

This latter point is one reason why the collection angle of the spectrometer, β, is so important.

Also you must remember to distinguish between the definitions of scattering that will keep appearing.

- *Single scattering* occurs when each electron undergoes at most one scattering event as it traverses the specimen.
- *Plural (>1* and *< 20) scattering* implies that the electron has undergone a combination of interactions and lost energy from some or all of them.
- *Multiple (> 20) scattering* only occurs in very thick specimens or with very low energy electrons, so is irrelevant to TEM.

We'll see that the energy-loss spectrum is most understandable and more easily modeled when we can approximate everything to single scattering. This ideal is approached when we have a combination of very thin specimens and high accelerating voltages. In practice, most specimens are thicker than ideal and so we usually acquire plural-scattering spectra and we may have to remove the plural-scattering effects via deconvolution routines which are available in commercial and free EELS software packages (see URLs #1–3). We'll address the general topic of spectral simulation and manipulation later and in more depth in the companion text. We've already told you about deconvoluting out the PSF in Chapter 37, we'll see in Section 38.2.B, that you can do similar things if you want to remove the ZLP, and removing plural-scattering effects in high-loss spectra will be discussed in Section 39.6.

DECONVOLUTION WARNING

Whenever we mention deconvolution (and we'll do so quite often), remember that there is the danger of introducing artifacts into the part of the spectrum that you have just tried to simplify.

Typical energy losses: The principal inelastic interactions in order of increasing energy are phonon excitations, interband and intraband transitions, plasmon excitations, and inner-shell ionizations. We've already introduced these processes back in Chapter 4. The energy loss $\mathcal{E}$ of the principal scattering processes that we study in EELS are single-electron scattering (inter/intraband transitions), 2–20 eV, plasmon interactions 5–30 eV, and inner-shell ionizations, 50–2000 eV. Phonon excitations cause losses of $\sim$ 0.02 eV so, even with the best energy resolution in monochromated AEMs, it's not possible to separate these from the ZLP, although the phonon-scattering angle can be quite large and (particularly for heavier elements) these electrons can be seen as the background intensity between the principal spots in an SAD pattern. But that's about all we'll say about phonon scattering, except that you should be able to work out why cooling your specimen will help to reduce their presence. We'll deal with the first three (low-loss) processes in this chapter and the ionization (high-loss) process in the next chapter. There are also ionization events with energy losses >2 keV but it is difficult to detect these because the signal is relatively weak and, at such energies, the X-ray signal is strong, so we tend not to do much EELS > 2 keV.

REMEMBER θ

The symbol θ in all cases refers to the scattering *semi*-angle even if we just say angle.

THE MOST IMPORTANT ANGLE IS θ_E

The so-called characteristic or most-probable scattering angle (for an energy loss $\mathcal{E}$)—it depends on the beam energy.

Typical scattering angles: It's a little difficult to be specific about the values of scattering angle, θ, because the angle varies with beam energy and the energy-loss process. We always assume that the scattering is symmetrical around the direct beam and there are two principal scattering angles that you should know. You can find derivations of the equations in Egerton's text.

$$\theta_E \approx \frac{\mathcal{E}}{2E_0} \tag{38.1}$$

If the beam energy is in eV the angle is in radians. This equation is an approximation (good to about ±10%) and it ignores relativistic effects and doesn't work for phonons, so you should only use it for rough calculations and be particularly suspicious above ~100 keV. We can be more precise and define θ_E as

$$\theta_E \approx \frac{\mathcal{E}}{(\gamma m_0 v^2)} \tag{38.2}$$

Here we have the usual definitions: m_0 is the rest mass of the electron, v is the electron velocity and γ is given by the usual relativistic equation (where c is the velocity of light)

$$\gamma = \left(1 - \frac{v^2}{c^2}\right)^{-\frac{1}{2}} \tag{38.3}$$

The other useful angle θ_c is the cut-off angle above which the scattered intensity is zero

$$\theta_c = (2\theta_E)^{\frac{1}{2}} \tag{38.4}$$

Be careful to calculate θ_c in radians, not milliradians. Knowing the characteristic scattering angle is obviously important if you want to gather an intense spectrum highlighting a particular energy loss. For example, a plasmon interaction with 100-keV electrons, causing a typical energy loss of 20 eV will have a characteristic scattering angle of ~0.1 mrads. Using a smaller β will cut off intensity in the spectrum which is why we told you in the last chapter to ensure that $\beta > 2–3\theta_E$. Knowing the cut-off angle (which is typically an order of magnitude greater than the characteristic angle at 100 keV) will give you a maximum useful value of β. If you use too large a value of β then there's the chance that you'll get unwanted electrons in the spectrum

(e.g., diffracted beams) but you've got to try really hard to encounter this problem.

38.2 THE ZERO-LOSS PEAK (ZLP)

38.2.A Why the ZLP Really Isn't

If your specimen is thin enough for EELS, the predominant feature in the spectrum will be the ZLP, as shown in Figure 38.1. As the name implies, the ZLP consists primarily of electrons that have retained the incident-beam energy E_0. Such electrons may be forward scattered in a relatively narrow cone within a few mrads of the optic axis and constitute the 000 spot in the DP, i.e., the direct beam. If you were to tilt the incident beam so a diffracted beam entered the spectrometer then it, too, would give a ZLP.

MAGNITUDE OF ANGLES

The scattering angles for diffraction ($2\theta_B$) are relatively large (~20 mrad) compared to the smaller scattering angles in EELS. So the diffracted beams will only enter the spectrometer if you select them.

Actually, we can also measure the intensity and energy of electrons as a function of their angular distribution, and we'll discuss angular- or momentum-resolved EELS later, in Section 40.8.

Now the term ZLP is really a misnomer for two reasons. First, as we've seen, the spectrometer has a finite energy resolution (at best ~ 0.3 eV without monochromation) so the ZLP will also contain electrons that have energy losses below the resolution limit, which are mainly those that excited phonons. This is not a great loss since phonon-scattered electrons don't carry useful information; they only cause the specimen to heat up. However, it does explain why we shouldn't really call this the ZLP. Second, we can't produce a monochromatic (single-color, i.e., single-wavelength/energy) beam of electrons; the beam has a finite energy range about the nominal value E_0 (at best 10–100 meV even with a monochromator). Despite this imprecision, we will continue to use the term zero loss.

From a spectroscopist's point of view, the ZLP is more of a problem than a useful feature in the spectrum because, as we mentioned in the previous chapter, it is so intense that it can saturate the PDA or the CCD detector, creating a ghost peak. So if you don't need to collect the ZLP in the spectrum then deflect it off the detector (or use the attenuator in the Gatan system). Conversely, from the microscopist's standpoint, as we'll see, selecting the ZLP to form an image or DP from which most of the energy-loss electrons have been excluded is a *very* useful technique. Conversely (again) filtering out the ZLP and forming images with selected energy-loss electrons is also extraordinarily useful.

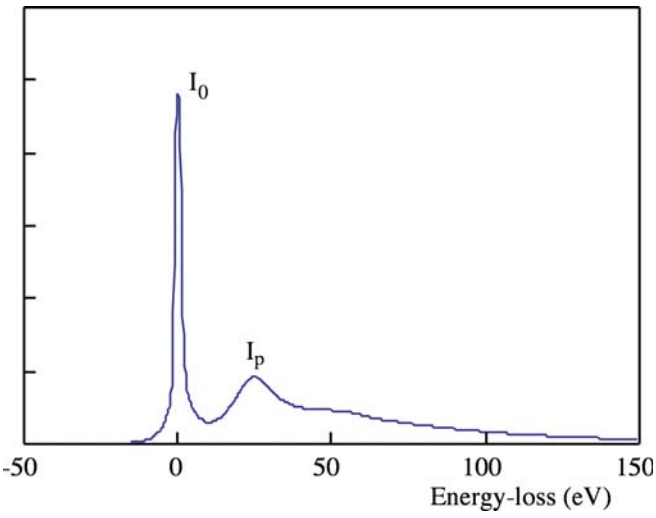

FIGURE 38.1. The low-loss spectrum showing an intense ZLP. The next most intense peak is a plasmon peak and the rest of the spectrum out to the high-loss (> 50 eV) region is relatively low intensity.

38.2.B Removing the Tail of the ZLP

The intense ZLP has a tail, either side of it (go back and look at Figure 37.4), ultimately limited by the energy resolution. On the low (negative) energy side of the peak, the point-spread function accounts for the tailing, but on the high (positive) energy side there are contributions from the low-loss (e.g., phonon) electrons we just discussed. It is sometimes necessary to remove this tail before studying the (very) low-loss spectrum, e.g., for dielectric-constant determination (see Section 38.3). There are various ways to remove this tail in Gatan's commercial software (e.g., comparison with reference spectra, subtraction versus deconvolution) and the software continues to improve. You must make sure you are displaying the spectrum with a high dispersion and deconvolute the point-spread function before doing anything else.

The best way to remove the tail, if you *really* need to study the spectrum close to the ZLP, is to use a monochromator and cut off the tail of the peak at the source, so that any intensity outside the ZLP is a true low-loss part of the spectrum. In this particular case, since the low-loss spectrum is relatively intense, the principal argument against monochromation (i.e., you throw away a lot of expensive electrons) is seriously weakened. We've already mentioned this in Section 37.7 and Figure 37.16 compares the energy spread in the ZLP before and after monochromation.

If you don't have a monochromator, removal of the ZLP peak is challenging and prone to artifacts. The

main problem is that the shape of the ZLP measured with the beam on the specimen is not always the same as the ZLP measured in the hole because of phonons and elastic-scattering effects.

38.2.C Zero-Loss Images and Diffraction Patterns

If we filter out all the electrons which have lost energy greater than the resolution of the spectrometer (typically $> \sim 1$ eV) then basically we have an elastic image or DP. In doing this we immediately remove chromatic-aberration effects from the image, since it is the imprecise focusing of energy-loss electrons that degrades the resolution of TEM images from thick specimens. You should go back and take a look at Section 6.5.B and equation 6.16 and you'll see that, if many electrons suffer a typical (e.g., plasmon) $\mathcal{E}$ of $\sim$15 eV, your image resolution degrades from a few Å to several nanometers. For such $\mathcal{E}$ to occur, the specimen thickness has to be a goodly fraction of the plasmon mean free path (see Table 38.1), but that is not unusual. In addition to degrading the resolution by adding a diffuse component to otherwise focused TEM images, the energy-loss electrons also account for the diffuse intensity between spots in DPs. So filtering out these electrons should both increase the image contrast and improve the quality of the DPs.

The positive effect of energy filtering on resolution and *all* forms of TEM-image contrast has been known for several decades (see Egerton's early papers). This technique is particularly useful for enhancing the quality of images from thick biological (or polymeric) specimens in which the inelastic scattering is stronger than the elastic scattering (see Figure 38.2). However, diffraction contrast can also be enhanced by filtering of images from thick specimens (see Figure 38.3) but also in thin specimens because inelastically scattered electrons broaden the excitation error, **s**, thus reducing diffraction contrast. Sometimes enhancement of mass-thickness contrast images can be achieved by 'tuning' the spectrometer to select a specific range of energies (Figure 38.4). Contrast tuning (see Egerton's text) involves selecting an energy-loss window and sliding it around the spectrum while watching the image to find the best contrast. Tuning is useful in both the low and high-loss regions of

TABLE 38.1 Plasmon-Loss Data for 100-keV Electrons for Several Elements (from Egerton, 1996)

Material	$\mathcal{E}_P$ (calc)(eV)	$\mathcal{E}_P$ (expt)(eV)	θ_E(mrad)	θ_C(mrad)	λ_P(calc) (nm)
Li	8.0	7.1	0.039	5.3	233
Be	18.4	18.7	0.102	7.1	102
Al	15.8	15.0	0.082	7.7	119
Si	16.6	16.5	0.090	6.5	115
K	4.3	3.7	0.020	4.7	402

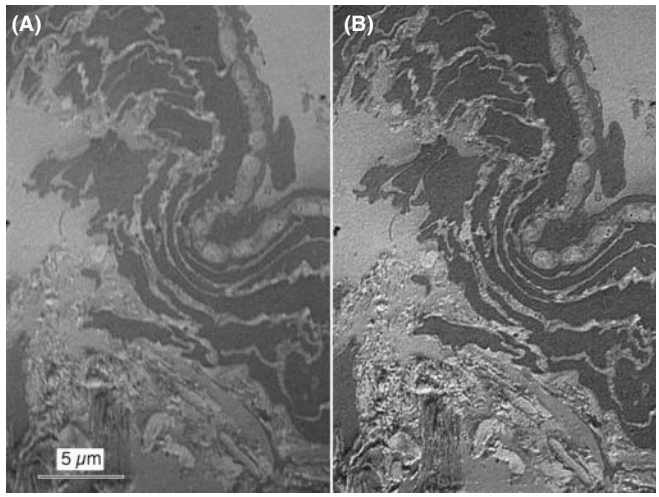

FIGURE 38.2. Comparison of (A) unfiltered and (B) filtered image of a thick biological section showing the enhanced contrast and resolution when the energy-loss electrons are removed.

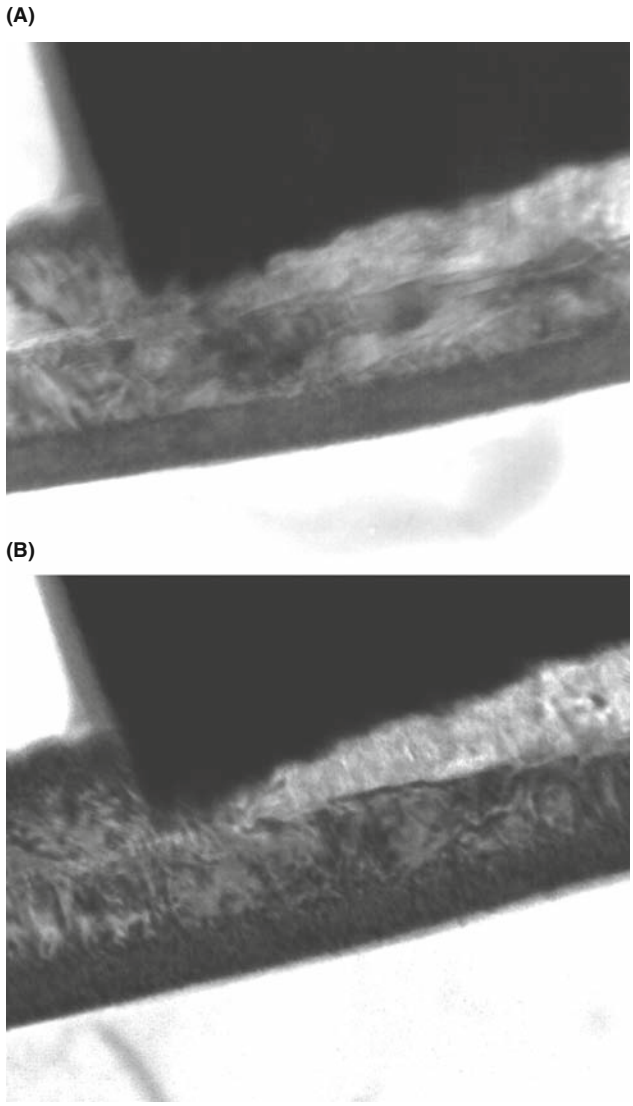

FIGURE 38.3. Comparison of (A) unfiltered and (B) filtered image of a thick crystalline specimen showing enhanced diffraction contrast when the energy-loss electrons are removed.

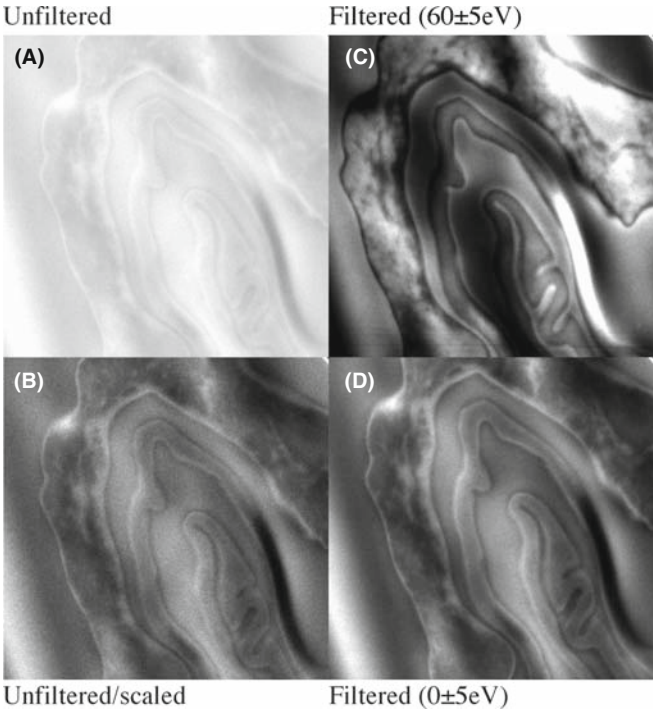

FIGURE 38.4. Contrast tuning of an image from a thick biological specimen to determine the region of the low-loss spectrum that gives the optimum contrast. (A) Unstained mouse epidermis (thickness = 0.1 μm, 100 keV). (B) Unfiltered image, digitally scaled to show the best contrast. (C) Filtered, contrast-tuned at 60±5 eV; the image has much better contrast than (B). (D) Filtered, contrast-tuned at 0±5 eV; the image has improved resolution and better contrast (B), but not as strong contrast as (C). Full width = 1 μm.

the spectrum and is typically done anywhere from 0 to 200 eV. As shown in Figure 38.4, there is significant possibility for contrast improvement in the low-loss region. In the high-loss region, selecting an energy window before an edge tends to reduce contrast from the edge electrons while windows after an edge tend to enhance contrast from the edge (see also jump-ratio imaging in Section 39.9).

High-resolution phase-contrast images (from thin specimens) should be more easily compared with theory if they are filtered to remove the diffuse background because we won't need so many 'fudge factors.' (See Chapter 28.) For a given thickness of specimen, the only alternative to reducing chromatic aberration is to go to higher voltages and this is perhaps an even more expensive option than buying a filter!

As we discussed back in Sections 37.8 and 20.5, if the energy-loss electrons are removed from SADPs and CBDPs it makes them much clearer (e.g., the paper by Midgley et al. and Reimer's chapter in Ahn's text), as shown back in Figures 20.10 and 37.17C. Energy filtering can also reveal extra diffraction information, such as the radial-distribution function for amorphous materials, which we'll tell you about later in Section 40.7.

If you've got a thick (several tens of nm) specimen (which is sometimes all you can manage to create), filtering may give many improvements

- Filtering can improve the image resolution.
- Filtering can enhance the image contrast no matter what mechanism is operating.
- Filtering can improve the contrast in diffraction patterns.
- Filtering can reveal finer detail in images and DPs.

So it would be really great if we could leave the filter switched on all the time, but this isn't always practically feasible.

Perhaps what is more surprising is why, given the tremendous advantage of filtering, simple zero-loss filters haven't been commercially available for decades? One experimental problem is that the energy-loss spectrometer is susceptible to external fields and the ZLP shifts over time, making continuous EFTEM imaging difficult: you have to continually re-align and re-focus the ZLP. Also, the best results, particularly for quantitative imaging (see the next chapter), require that your specimen has a similar thickness over the entire area of the image and that strong diffraction effects are minimized. Another possible reason is that filtering works best for thick specimens, which don't permit the TEM to perform at its (spherical-aberration) resolution limit of a fraction of a nanometer. It is perhaps not advantageous to remind users that most of their specimens are such that their TEM can't deliver anything like its best resolution, and that buying a 'better' TEM will have no beneficial effect on image quality or resolution for the great majority of (thick) specimens. But of course, this is only speculation. . .!

38.3 THE LOW-LOSS SPECTRUM

Look again at Figure 38.1, which is a typical low-loss spectrum and several points are immediately obvious

- After the ZLP, the plasmon peak is the next major peak.
- Apart from the plasmon, the spectrum is relatively featureless (the intensity changes are small).
- Despite the lack of features, there's still a lot of counts (check the units of the ordinate), so extracting useful data is still feasible and imaging should be relatively straightforward.

The cut-off energy for the low-loss spectrum, as we've already noted, is $\sim$ 50 eV and the reason for this is that the other principal features of energy-loss spectra, namely, the ionization edges, don't appear (at least for solids) until $\mathcal{E} > 50$ eV. In the low-loss spectrum, we

are detecting beam electrons that have interacted with conduction and/or valence bands (hence another common term for the low-loss spectrum is 'valence spectrum'). These weakly bound electrons control many electronic properties of the specimen. In general, the low-loss spectrum is not as well understood as the high-loss spectrum and there has not been the same effort put into modeling low-loss spectra, as we'll describe for the higher-loss spectra in Chapters 39 and 40. However, things are beginning to change, as you'll see later in this chapter.

While we have just shown you the tremendous advantages of filtering out the plasmon peak in order to enhance contrast and resolution in TEM images and DPs, there is also much to be gained by imaging the plasmon peak and filtering out the ZLP and high-loss electrons. This approach was pioneered by Batson. Because of the strength of the signal, plasmon imaging is becoming a much more popular technique, particularly for mapping out low-loss properties of nanomaterials (e.g., see the papers by Eggeman et al. and by Ding and Wang).

38.3.A Chemical Fingerprinting

So what can we do with the low-loss spectrum? Because there are a lot of counts, we can use the shape of the spectrum to help identify specific phases or features in the TEM image with some degree of statistical certainty. The low-loss spectrum all the way up to ~50 eV, including any plasmon peaks (see Section 38.3.C), should be used for fingerprinting.

FINGERPRINTING

The low-loss spectrum can only be used for phase identification through a 'fingerprinting' process. You store the spectra of known specimens in a library in the computer.

So you overlay your unknown spectrum on one or more stored library-standard spectra. Figure 38.5 shows how low-loss spectra vary (A) for aluminum and various compounds and (B) for the main constituents of biological specimens. A collection of low-loss spectra from many elements and common compounds (mainly oxides) has been compiled in various databases, such as the EELS Atlas or on the Web at URL #4. Such sources can help considerably with fingerprinting unknown features in your image. As with any fingerprinting technique, including the forensic variety, you must be careful to decide when a 'match' is satisfactory. There is no 'black and white' here, only shades of gray, so don't convict unless the statistics are with you and there is strong supporting evidence from other techniques.

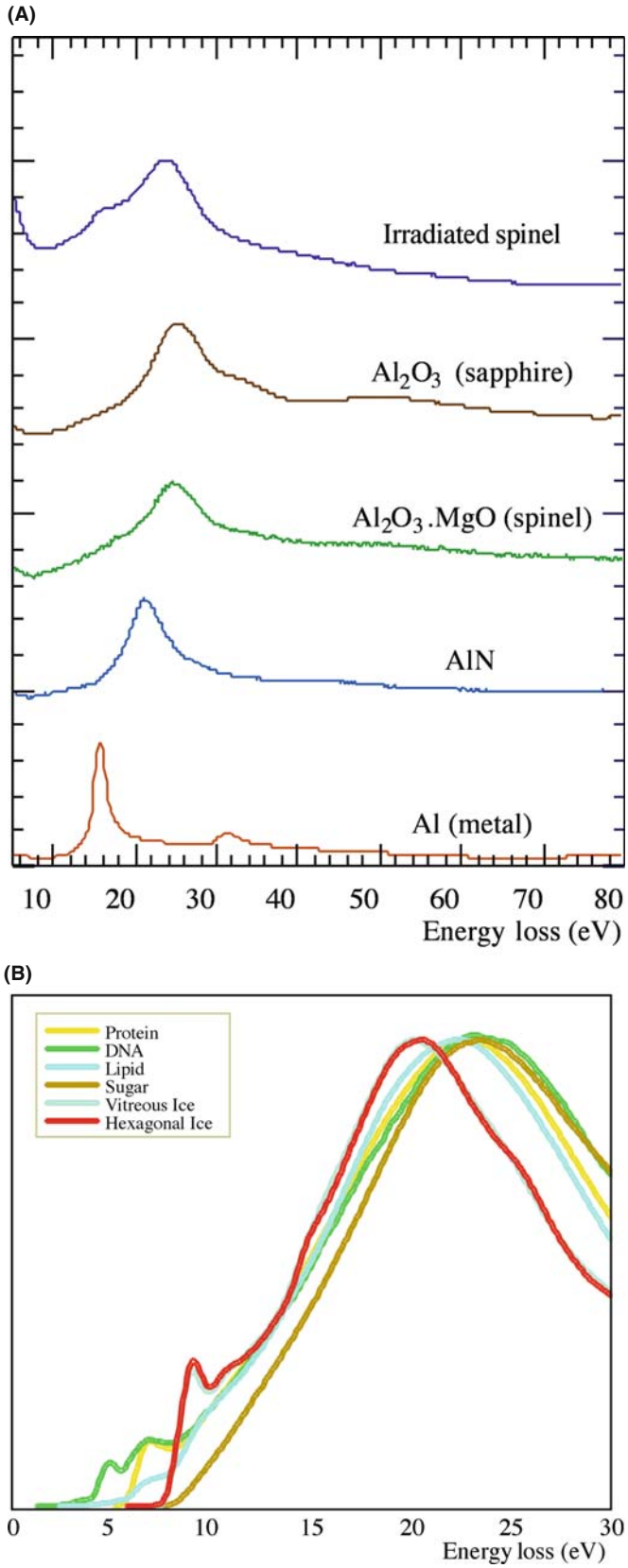

FIGURE 38.5. (A) The low-loss spectrum from specimens of Al and various compounds, showing differences in the intensity variations that arise from differences between the Al-Al, Al-O, and Al-N bonding. (B) Low-loss spectra from the principal components of cellular tissue.

38.3.B Dielectric-Constant Determination

We can view the energy-loss process as the dielectric response of the specimen to the passage of a fast electron. As a result, the very low energy spectrum (up to $\mathcal{E} \sim 20$ eV) contains information about the dielectric constant or permittivity (ε). Localized dielectric-constant measurements are of great interest as the semiconductor industry explores high-dielectric materials, such as HfO_2, for the next generation of nanometer-scale gate oxides.

Assuming a free-electron model, the single-scattering spectrum intensity $I(\mathcal{E})$ is related to the imaginary (Im) part of the dielectric constant ε by the expression (modified from Egerton)

$$I(\mathcal{E}) = I_0 \frac{t}{k} \mathrm{Im}\left(-\frac{1}{\varepsilon}\right) \ln\left[1 + \left(\frac{\beta}{\theta_E}\right)^2\right] \qquad (38.5)$$

where I_0 is the intensity in the ZLP, t is the specimen thickness, k is a constant incorporating the electron momentum and the Bohr radius, β is the collection angle (again note its importance), and θ_E is the characteristic-scattering angle. You can use a Kramers-Kronig analysis to analyze the energy spectrum in order to extract the real part of the dielectric constant from the imaginary part in equation 38.5 and details are given in Egerton's text. As usual, the advantage to doing this kind of measurement in the TEM is the high spatial resolution and the advantages of this are exemplified by the use of low-loss spectroscopy to determine optical gaps on BN nanotubes (Arenal et al.). Since you need a single-scattering spectrum, removing the plural scattering intensity by Fourier-logarithmic deconvolution is the first step (see Section 39.6) when determining the dielectric constant. The Gatan software package has the appropriate programs and public-domain software is also available, e.g., URLs #1, 5, and 6.

KRAMERS-KRONIG ANALYSIS
This analysis gives the energy-dependence of the dielectric constant and other information, which we usually obtain by optical spectroscopy.

The alternatives to EELS for this kind of work are various kinds of optical and other electromagnetic-radiation techniques. The part of the low-loss spectrum from ~1.5 to 3 eV is of great interest and corresponds to optical analysis of the dielectric response from the infra-red (~800 nm) through the ultra-violet (~ 400 nm) wavelength range. (This correspondence between EELS and optical spectroscopy only holds for small angles of scattering so the value of β you choose must be small (< ~ 10 mrads) thus lowering the intensity in the spectrum.) Higher energies correspond to various electronic transitions. Thus, in a single EELS experiment you can, in theory, substitute for a whole battery of optical-spectroscopy instrumentation (although optical spectroscopy techniques do offer even better energy resolution than EELS). Remember that EELS always offers better spatial resolution.

There is a tremendous similarity between the TEM-EELS approach and the valence (surface) EELS approach, including the need for Kramers-Kronig and deconvolution software. TEM-based EELS is in the extremely low-energy (i.e., low-frequency) range around 1 eV and below and corresponds to far infra-red spectroscopy which is well into the energy range of studies of bond vibrations. Higher up the energy-loss range corresponds to the visible and ultra-violet ranges.

If you don't have access to a monochromator, you can use software to remove the contribution of the tail of the ZLP but, as we mentioned above, be careful, because this process may introduce its own artifacts. An example of the correspondence between EELS and optical valence spectra is shown in Figure 38.6. In Figure 38.6A, the importance of initial deconvolution is demonstrated and the deconvoluted valence spectra are compared with ultra-violet spectra in Figure 38.6B. It is straightforward to assign the various peaks in the low-loss spectra to specific interband transitions and also to compare the data with band-structure calculations (e.g., van Bentham et al.). Thus, the electronic and optical properties can be obtained and you can, of course, select any of the features in the low-loss spectrum and form images with those electrons. So dielectric-constant imaging is feasible, as is imaging the various other low-loss signals which we'll now discuss.

FOR THE BEST LOW-LOSS SPECTROSCOPY
You need an FEG, a high-resolution, high-dispersion spectrometer and if you're really going to do it properly, a monochromator, so the tail of the ZLP does not mask the low-energy intensity.

38.3.C Plasmons

Plasmons are longitudinal wave-like oscillations that occur when a beam electron interacts with the weakly bound electrons in the conductance or valence band. You can think of plasmons as being like the ripples that spread out from where a pebble is dropped into a pond. But, unlike in a pond, the oscillations are rapidly damped, typically having a lifetime of about 10^{-15} s and so are quite localized to <10 nm. The plasmon peak is the second most dominant feature of the energy-loss spectrum after the ZLP. The small peak beside the ZLP in Figure 38.1 is a plasmon peak.

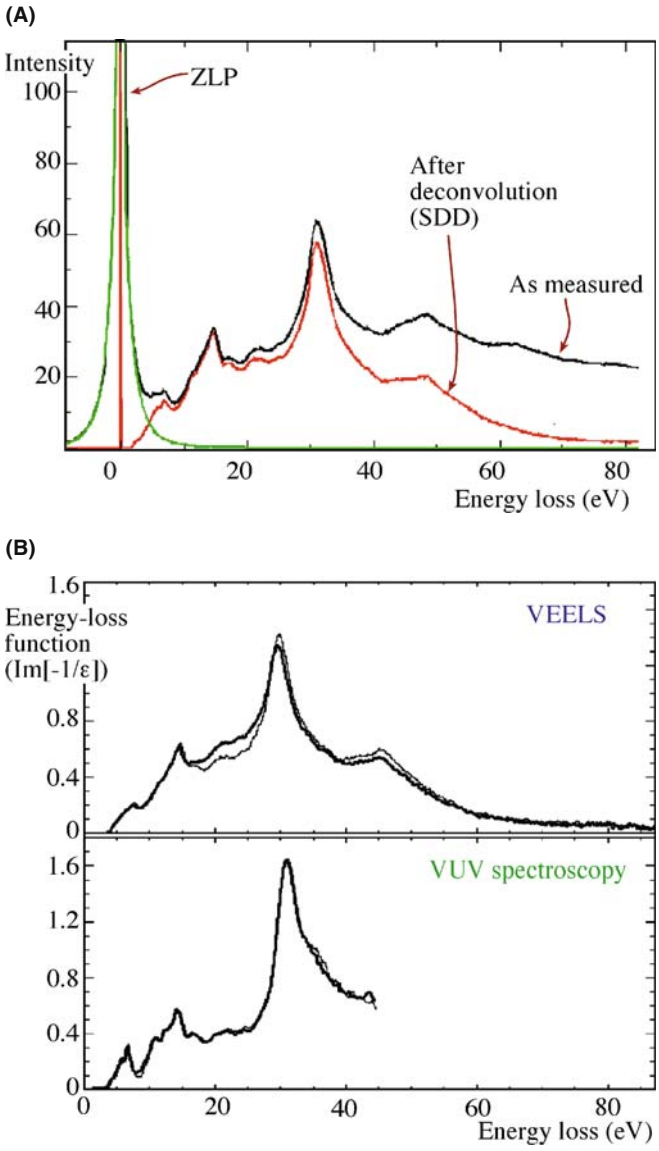

FIGURE 38.6. (A) Low-loss (valence) spectrum from $SrTiO_3$ before (black) and after (red) Fourier-log deconvolution. The extracted ZLP is shown in green. (B) Comparison of the change in the imaginary part of the complex dielectric function obtained from pairs of valence EELS (VEELS) spectra and valence ultra-violet (VUV) spectra from two different regions of $SrTiO_3$. The spectra show similar features but the VUV spectrum cannot be measured beyond ~ 45 eV.

If we assume the electrons are free (i.e., not bound to any specific atom or ion), then the energy $\mathcal{E}_P$ lost by the beam electron when it generates a plasmon of frequency ω_p is given by a simple expression

$$\mathcal{E}_P = \frac{h}{2\pi}\omega_p = \frac{h}{2\pi}\left(\frac{ne^2}{\varepsilon_0 m}\right)^{\frac{1}{2}} \qquad (38.6)$$

where h is Planck's constant, e and m are the electron charge and mass, ε_0 is the permittivity of free space (remember the dielectric constant is the relative permittivity of a polarizable medium), and n is the free-electron density. Typical values of $\mathcal{E}_P$ are in the range 5–25 eV and a summary of plasmon-loss characteristics is given in Table 38.1

- Plasmon losses dominate in materials with free-electron structures, such as Li, Na, Mg, and Al.
- Plasmon-like peaks occur to a greater or lesser extent in the low-energy spectra from all materials, including insulators, such as polymers and biological tissue.

So the 'free-electron' assumption is clearly not rigorous and we don't know everything about how this feature arises.

From equation 38.6, you can see that $\mathcal{E}_P$ is affected by n, the free-electron density. Interestingly, n may change with the chemistry of the specimen. Thus, measurement of the plasmon-energy loss can give indirect analytical information (see the next section).

The characteristic plasmon-scattering angle θ_E is very small, being typically < 0.1 mrads (as listed in Table 38.1), which means that the plasmon-loss electrons are strongly forward scattered. Their cut-off angle $\theta_{c\ is}$ much greater than θ_E so if you use a collection angle β of only 10 mrads, you will easily gather almost all the plasmon-loss electrons (again note the importance of knowing β in your system). Conversely, this means that even a small objective aperture will not stop plasmon-loss electrons entering the TEM imaging system. Plasmon-loss electrons also carry contrast information and, because they are the most intense energy-loss signal, they are the primary contribution to chromatic aberration in TEM images, which is why it is often a good move to filter them out. As we've already seen, Figure 38.2 shows the improvement in image contrast and resolution when the low-loss (primarily plasmon) spectrum is filtered out of the image of a specimen showing predominantly mass-thickness contrast. Likewise, Figure 38.3 shows a thick foil exhibiting primarily diffraction contrast. A similar improvement in resolution occurs when the many plasmon peaks are filtered out.

A typical value of the plasmon mean free path λ_P at AEM voltages is about 100 nm and so it is reasonable to expect at least one strong plasmon peak in all but the thinnest specimens. Likewise, the number of individual losses should increase with the thickness of your specimen and we can use the plasmon-peak intensity to estimate the specimen thickness. If indeed your specimen is so thin that only single scattering occurred, and the only significant scattering was a single plasmon event, then you should be very pleased because it's a great specimen for ionization-loss EELS (see the next chapter). Conversely, if your spectrum shows several plasmon peaks then it is too thick for ionization-loss studies. Under single-scattering circumstances we can assume

$$t = \lambda_p \frac{I_p}{I_0} \qquad (38.7)$$

where λ_P is the plasmon mean free path, I_P (see Figure 38.1) is the intensity in the first (and only) plasmon peak, and I_0 is the intensity in the zero-loss peak.

BALLPARK CALCULATION

A typical ballpark figure: if the intensity in the first plasmon peak is greater than one tenth the zero-loss intensity then your specimen is too thick for EELS quantification.

The method has advantages over other thickness measurement techniques in that you can apply it to any specimen, amorphous or crystalline, over a wide range of thicknesses. We'll tell you more about EELS thickness measurements and their role in ionization-loss spectrometry in Section 39.5.

If plural scattering is significant, then the spectrum becomes more difficult to interpret and other problems arise; e.g., your ionization-loss quantification results (next chapter) become unreliable.

Of course, one way around this problem is to use very thin foils, but often you can't produce thin-enough specimens. Murphy's law says that the area you're interested in will usually be too thick. Then you have to deconvolute the spectra, again using the Fourier-log approach (Section 39.6) to make the single-scattering assumption valid. As we've already noted, deconvolution brings its own problems.

Figure 38.7 shows the plasmon-loss spectra from (A) thin and (B) thick foils of pure Al and (B) also indicates how the Gatan software uses this information to come up with a measure of the local foil thickness. Since Al is a good approximation to a free-electron metal, the plasmon-loss process is the dominant energy-loss event. Plural-plasmon scattering in thicker foils is of concern because it limits the interpretation of high energy-loss spectra containing chemical information from ionization losses in which we are really interested (see Section 39.4).

The plasmon losses which we've just described all arise from interactions with the electrons in the interior of your specimen, but the incident electrons can also set up plasmon oscillations on the specimen surface. We can envisage these surface plasmons as transverse charge waves. Surface plasmons have about half the energy of volume plasmons (because the surface atoms are not so strongly bound). Generally, however, the surface plasmon peak is much less intense than the volume plasmon peak(s), even in the thinnest specimens, but you can still use them for imaging, as shown by Batson. With monochromators and aberration correctors, studies of surface plasmons, along with other low-loss features, will assume more importance in the TEM.

38.3.D Plasmon-Loss Analysis

As we just mentioned, the plasmon peaks contain chemical information, because the composition of the specimen may affect the free-electron density, n, which in turn changes the plasmon-loss peak position. Historically, this technique was the first aspect of EELS to produce quantitative analysis data, and it was used in a limited number of systems, mainly aluminum and magnesium alloys in which the plasmon-loss spectrum is dominant and consists of sharp Gaussian peaks (Williams and Edington). The lack of a more recent review gives some indication of the limitations of this approach (see below)!

The principle of plasmon-loss analysis is based on empirical observation of the shift in the plasmon-peak position ($\mathcal{E}_P$) with composition (C), giving an expression of the form

$$\mathcal{E}_P(C) = \mathcal{E}_P(0) \pm C\left(\frac{d\mathcal{E}_P}{dC}\right) \qquad (38.8)$$

where $\mathcal{E}_P(0)$ is the plasmon loss for the pure component. By creating a series of binary alloys of known composition we can develop a working curve which we can then use to calibrate measurements of $\mathcal{E}_P$ in unknown alloys.

Since plasmon-loss analysis demands the measurement of peak *shifts* rather than peak positions, you need an energy spectrum of the highest resolution and sufficient dispersion to measure the peak centroid accurately. The early plasmon-loss studies did not have

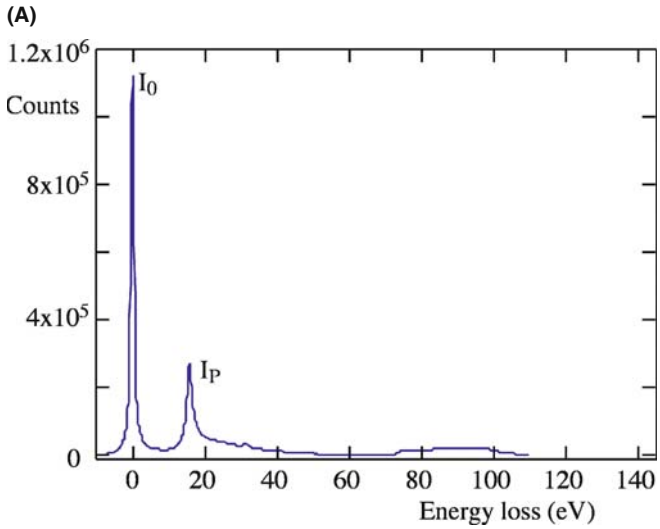

FIGURE 38.7. (A) The low-loss spectrum from a very thin specimen of pure Al showing the intense ZLP (I_0) and a small plasmon peak (I_P) at about 15 eV. (B) The low-loss spectrum from a thick specimen of pure Al showing several plasmon peaks, the first of which is almost as intense as the ZLP. The inset shows the calculation of the thickness from the Gatan software.

(B)

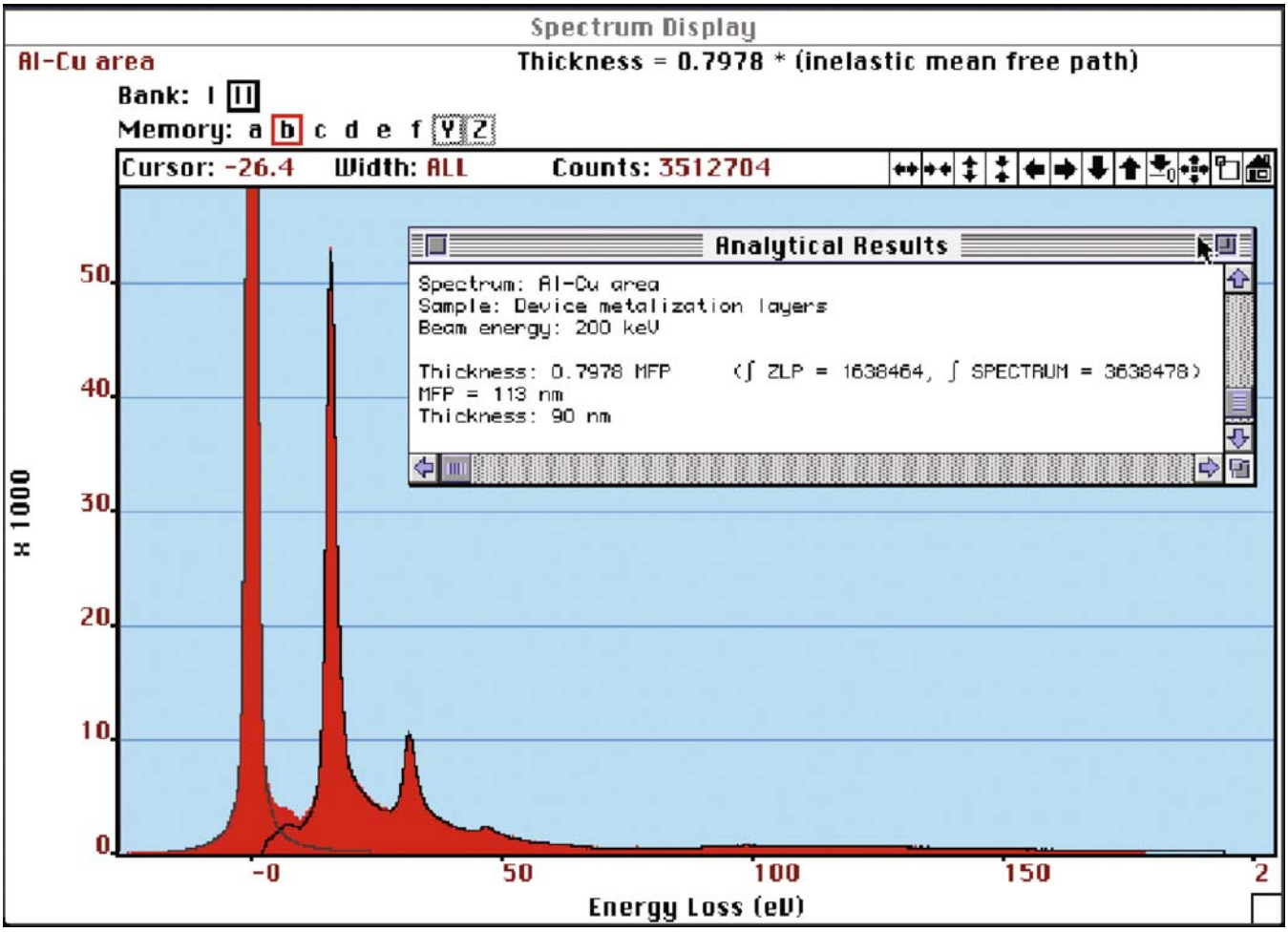

FIGURE 38.7. (Continued).

access to FEGs and so the resolution of the thermionic source was a limiting factor. Figure 38.8 illustrates some early plasmon-loss concentration data and the visible peak shifts that occur and also shows how we can use the plasmon peak shifts in Al-Li alloys and convert them into Li concentration data and also create Li compositions maps, which, given its low Z, is rather difficult to do with other analytical techniques.

Plasmon-loss spectrometry has reasonable spatial resolution and is relatively insensitive to specimen thickness and surface deposits. The spatial resolution is controlled by the localization of the plasmon oscillation which is only a few nm, since the plasmon disturbance is rapidly damped by the free electrons. The specimen thickness only affects the number and intensity of the plasmon peaks, not their position, as you can see in Figure 38.7. In fact you get the best results from plasmon-loss spectrometry when your specimen is about 1–2 mean free paths (λ_P) thick so that several, intense, Gaussian peaks are observable. There are, unfortunately, strong practical disadvantages, which account for the almost complete absence of plasmon-loss data since the advent of ionization-loss techniques in the mid-1970s

- We are limited to specimens showing well-defined peaks, and only binary specimens can be sensibly analyzed.
- The alloying element must produce a detectable change in $\mathcal{E}_P$ and this is not always the case. For example, the addition of 30 at.% Zn to Al scarcely changes $\mathcal{E}_P$.

It is possible that application of modern detection and data processing techniques may improve the quality and ease of analyzing plasmon-loss spectra. While plasmon peak-shift analysis is limited, we can at least use the low-loss plasmon spectra for chemical fingerprinting, as we've already described, and we'll discuss the prospects for more quantitative interpretation of low-loss spectra via modeling in Section 38.4.

With increasing interest in the mechanical properties of nanoscale materials, the fact that strong scaling

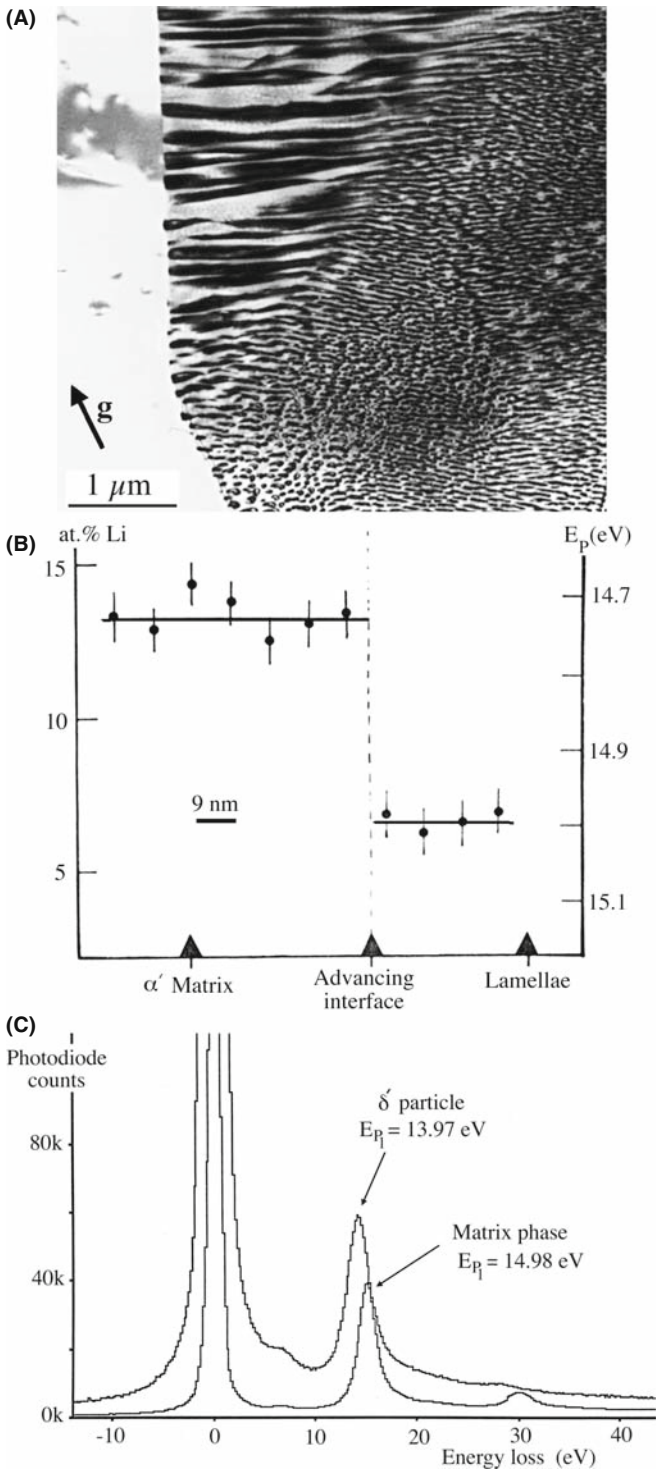

FIGURE 38.8. (A) A discontinuous precipitation reaction front in an Al-11 at.% Li specimen. (B) Experimental plasmon-loss measurements of the Li composition variation across the interface. (C) The shift in the plasmon peak for the matrix (5 at.% Li) and the precipitate (25 at.% Li) is clear in the two spectra.

correlations exist between the plasmon energy and elastic properties, hardness, valence-electron density, and cohesive energy is leading to a resurgence of interest in this part of the spectrum (e.g., Oleshko and Howe).

38.3.E Single-Electron Excitations

A high-energy beam electron may transfer sufficient energy to a single electron in the valence band to change its orbital state, perhaps moving it to an unoccupied state in the conduction band. We call these events single-electron interactions and they result in inter/intraband transitions for the valence electrons, with energy losses of up to ~25 eV. An example of an interband transition is given in the spectra from different polymers which can be distinguished solely by their electronic differences (Hunt et al.), as shown in Figure 38.9A. Interactions with molecular orbitals, such as the π orbitals produce characteristic peaks in this low-energy region of the spectrum, sometimes causing shifts in the plasmon peak (either up or down depending on the relative energy of the interband transition and the plasmon loss), and that is why it is possible to use the intensity variation in this part of the spectrum to fingerprint a particular phase. A more challenging example is given in Figure 38.9B, which shows what can be done with a combination of cryo- and low-dose STEM to image a polymer nano-emulsion in an aqueous medium. The low-loss spectra reveal the electronic differences between the phases (including amorphous ice!) and the filtered images show the lobed shape of the emulsified particles. There is probably no other technique that could image such beam-sensitive material at such high resolution (Kim et al.).

If a beam electron gives a weakly bound, valence-band electron sufficient energy to escape the attractive field of the nucleus, then a secondary electron (SE) is created, of the sort used to give topographic images in the SEM and STEM. Typically, a SE requires < 20 eV to escape the surface and therefore the electrons causing SE emission appear in the same low-energy region of the spectrum as the inter- and intraband transitions.

38.3.F The Band Gap

In the region of the spectrum immediately after the ZLP, and before the rise in intensity preceding the plasmon peak, you can see a region of low intensity. If there are no interband transitions occurring, the intensity in this portion of the spectrum approaches the dark-current (noise) level of the detector. This low intensity implies that there is a forbidden-transition region, which is simply the band gap, between the valence and conduction bands in semiconductors and insulators. To determine the band gap, you need to strip off the tail of the ZLP (with all the consequent difficulties) and measure the energy range of the gap out to the rise in the initial low-loss spectrum. Figure 38.10A illustrates the variable band gap in spectra from specimens of Si, and its oxide and nitride. Mapping this change in the energy range in which no transitions occur gives band-gap images (Figure 38.10B) and several examples of this are given by Kimoto et al. As sub-nanometer-scale semiconductor technology advances,

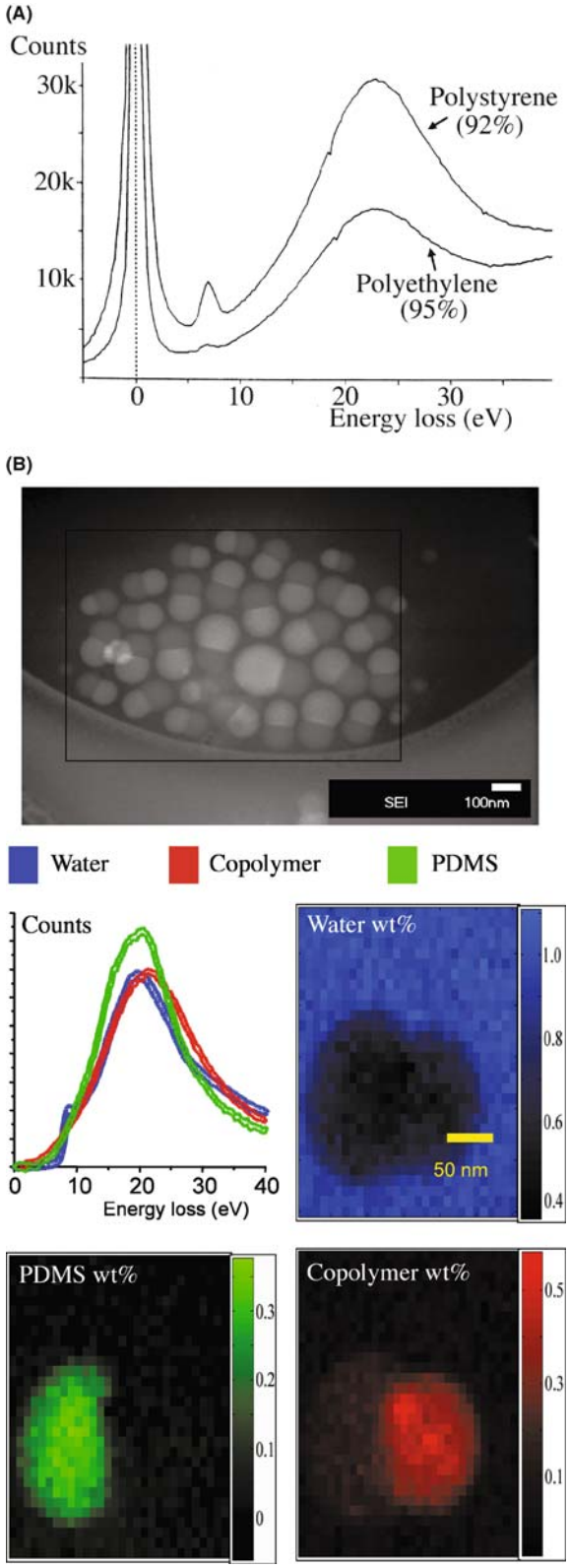

FIGURE 38.9. (A) The interband transition characteristic of polystyrene, clearly visible on the rise of the plasmon peak, compared with the absence of such a transition in polyethylene. (B) (top) A low-dose cryo-HAADF image of a two-phase polymer nano-emulsion in water; (bottom) low-loss spectra from amorphous ice (blue) polydimethyl siloxane (PDMS) (green) and a multi-phase co-polymer (red), together with the corresponding composition maps based on the differences in their low-loss spectra.

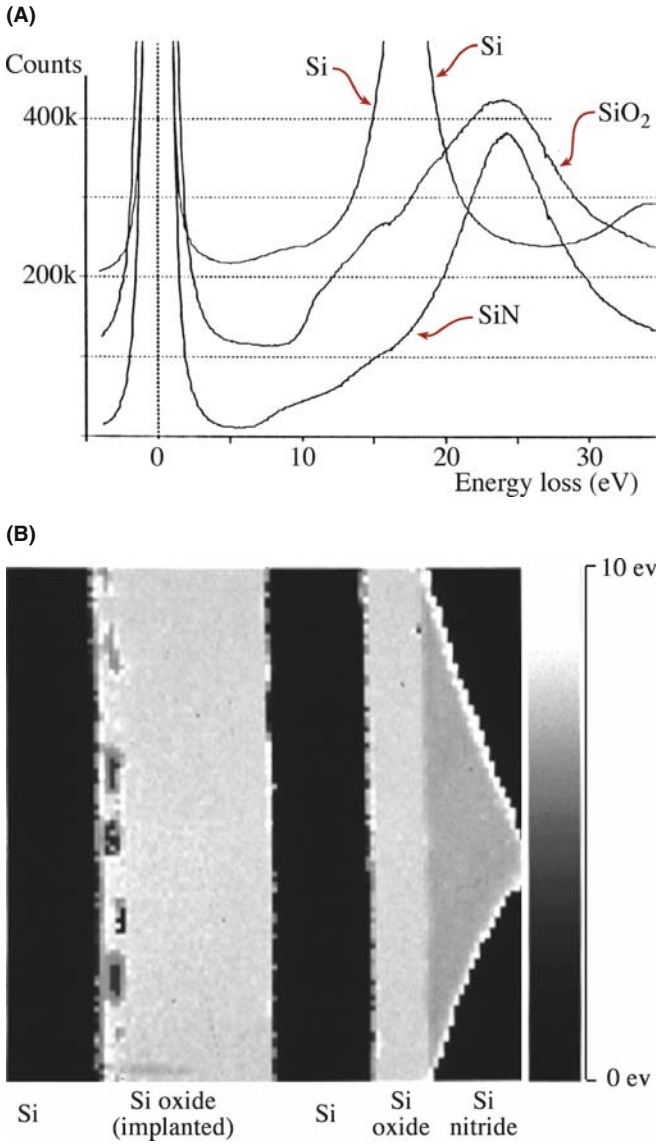

FIGURE 38.10. (A) Band-gap differences evident in the low-loss spectra of a Si semiconductor, SiO_2, and Si nitride (almost Si_3N_4) ceramic insulators and (B) the corresponding band-gap image (with scale on right; recorded at 90 K using 1024 channels and 150 ms dwell time). Note the Si islands in the oxide layer which were not visible in the TEM image.

the need for sub-nanometer resolution imaging of the band gap will increase and low-loss EEL images are the only way to visualize this electronic property.

38.4 MODELING THE LOW-LOSS SPECTRUM

As you now know, the low-loss spectrum has the advantage of significant intensity (so counting statistics are not a problem) and it contains useful data about your specimen, such as composition, bonding, the dielectric constant, the band gap, the free-electron density, and optical properties. With all this information you might have thought that we understood the spectrum very well and

were able to model it with some degree of precision and could use the modeling to predict spectra from different materials. Perversely, we are better able to do this for the much lower intensity, high-loss spectrum, as we'll describe in Chapters 39 and 40. However, significant progress is being made in calculating the plasmon-loss energies and interband transitions. As we've seen, the plasmon peak is basically an oscillation of the free electrons, so equation 38.6 has been used over several decades to calculate the plasmon-loss energy, but this approach can't handle the effects of other low-loss features like interband transitions. French has developed software for low-loss modeling, called Electronic Structure Tools (see URL #1), which consists of a number of programs for the quantitative analysis of optical, VUV, and EELS spectra. Keast has shown good agreement between experimental and calculated low-loss spectra for a range of metals and ceramics, as shown in Figure 38.11, using abinitio methods, which we'll describe in some more detail in Chapter 40, and this topic is dealt with extensively in the companion text. Modeling of such spectra requires careful experimental control and for the data of Figure 38.11 the convergence angle of the (100-kV) beam was 8.3 mrad, the Gatan spectrometer collection angle was 5.8 mrad, 100 spectra (0.05 s per acquisition) were aligned, corrected for dark current and gain variations, and summed. The density-functional theory (see Section 40.5.A) calculations (using the random-phase approximation and neglecting local-field effects) were performed using the WIEN2k code. Exchange and correlation effects were treated using the generalized gradient approximation. The final spectrum was averaged over the different orientation components. So you get the idea that this is not straightforward!

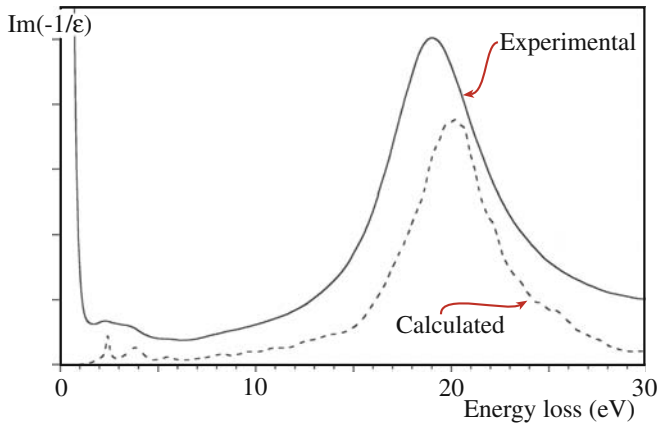

FIGURE 38.11. A comparison between the calculated (dashed) and experimental (full) low-loss spectrum from commercial MgB_2 particles.

Software for all aspects of low-loss analysis can be found at URLs #1 and 6.

CHAPTER SUMMARY

The low-loss (valence/plasmon) portion of the spectrum from 0 to 50 eV contains a wealth of useful information about the specimen.

- The ZLP is the most intense signal. If you filter out all the low-loss electrons apart from the ZLP, you get images and DPs which generally show higher resolution and better contrast than unfiltered ones because they are free of chromatic aberration and diffuse-scattering effects.
- The low-loss spectrum reflects beam interactions with loosely bound conduction and valence-band electrons.
- From different portions of the low-loss spectrum, you can measure the local dielectric constant of your specimen, the free-electron density, the thickness, the band gap, and observe inter/intraband transitions. You can also form images using energy-loss electrons which map out all these phenomena, generally with sub-nanometer resolution.
- The low-loss spectrum can be used to fingerprint (identify) specific elements, compounds, and biological tissue by comparison with the characteristics of standard spectra in databases.
- In some binary alloy systems of light elements, you can determine composition by measuring shifts in the plasmon-peak centroid. Plasmon imaging also has the potential for mapping nanoscale mechanical properties.
- We are getting much better at simulating the low-loss spectrum and understanding the various beam-specimen interactions that contribute to this high-intensity portion of the spectrum.

THE EELS ATLAS

Ahn, CC Ed. 2004 *Transmission Electron Energy-Loss Spectrometry in Materials Science and the EELS Atlas* 2nd Ed. Wiley-VCH Weinheim Germany. Buy this.

Ahn, CC and Krivanek, OL 1983 *EELS Atlas* Gatan Inc., 5933 Coronado Lane Pleasanton CA 94588. Buy this too (if you can find it).

SOME CALCULATIONS AND SPECIAL CONCEPTS

Egerton, RF 1976 *Inelastic Scattering and Energy Filtering in the Transmission Electron Microscope* Phil. Mag. **34** 49–65. One of the earliest indications of the power of EEL techniques.

Egerton, RF 1996 *Electron Energy Loss Spectroscopy in the Electron Microscope* 2nd Ed. Plenum Press New York. Includes the idea of high-contrast tuning.

Eggeman, AS, Dobson, PJ and Petford-Long AK 2007 *Optical Spectroscopy and Energy-Filtered Transmission Electron Microscopy of Surface Plasmons in Core-Shell Nanoparticles* J. Appl. Phys. **101** 024307–10.

Keast, VJ 2005 *Ab Initio Calculations of Plasmons and Interband Transitions in the Low-Loss Electron Energy-Loss Spectrum* J. Electron Spectrosc. Relat. Phenom. **143** 97–104.

Schattschneider, P and Jouffrey, B 1995 *Plasmons and Related Excitations* in Reimer, L Ed. *Energy-Filtering Transmission Electron Microscopy* 151–224 Springer New York. A thorough introduction to plasmons and related excitations.

APPLICATIONS

Arenal, R, Stéphan, O, Kociak, M. Taverna, D. Loiseau, A and Colliex, C 2005 *Electron Energy Loss Spectroscopy Measurement of the Optical Gaps on Individual Boron Nitride Single-Walled and Multi-walled Nanotubes* Phys. Rev. Lett. **95** 127601–127604.

Batson, PE 1982 *Surface Plasmon Coupling in Clusters of Small Spheres* Phys. Rev. Lett. 49 936–940.

Ding, Y and Wang, ZL 2005 *Electron Energy-Loss Spectroscopy Study of ZnO Nanobelts* J. Electr. Microsc. **54** 287–291.

Hunt, JA, Disko, MM, Behal, SK and Leapman, RD 1995 *Electron Energy-Loss Chemical Imaging of Polymer Phases* Ultramicrosc. **58** 55–64.

Kim, G, Sousa, A, Meyers, D, Shope, M and Libera, M 2006 *Diffuse Polymer Interfaces in Lobed Nanoemulsions Preserved in Aqueous Media* J. Am. Chem. Soc. **128** 6570 –6571.

Kimoto, K, Kothleitner, G, Grogger, W, Matsui, Y and Hofer F 2005 *Advantages of a Monochromator for Bandgap Measurements Using Eelectron-Loss Spectroscopy* Micron **36** 185–189.

Midgley, PA, Saunders, M, Vincent, R and Steeds, JW 1995 *Energy-Filtered Convergent-Beam Diffraction: Examples and Future Prospect*s Ultramicrosc. **59** 1–13.

Oleshko, VP and Howe, JM 2007 *In Situ Determination and Imaging of Physical Properties of Metastable and Equilibrium Precipitates Using Valence Electron Energy-Loss Spectroscopy and Energy-Filtering Transmission Electron Microscopy* J. Appl. Phys. **101** 054308–11.

Reimer, L 2004 *Electron Spectroscopic Imaging* in *Transmission Electron Energy Loss Spectrometry in Materials Science and the EELS Atlas* 2nd Ed. 347–400 Ed. CC Ahn Wiley-VCH Weinheim Germany.

Van Bentham, K, Elsasser, C and French, RH 2001*Bulk Electronic Structure of SrTiO3: Experiment and Theory* J. Appl. Phys. **90** 6156–6159.

Williams, DB and Edington, JW 1976 *High Resolution Microanalysis in Materials Science Using Electron Energy Loss Measurements* J. Microsc. **108** 113–145. Historical but not superceded!

URLs

1) http://www.lrsm.upenn.edu/∼frenchrh/index.htm
2) http://www.hremresearch.com/Eng/download/documents/EELScatE2.html
3) http://www.gatan.com/answers2/index.php
4) http://www.cemes.fr/%7Eeelsdb/
5) http://www.cemes.fr/epsilon/home/main.php
6) http://www.deconvolution.com/

SELF-ASSESSMENT QUESTIONS

Q38.1 Distinguish the low-loss and high-loss regions of the spectrum.
Q38.2 What is usually the second most intense peak in any spectrum? What might be the second most intense peak in a spectrum from a very thick specimen?
Q38.3 List the characteristic scattering angles of the principal energy-loss processes and give ballpark values. How do these compare with other important scattering angles in TEM such as typical Bragg angles?
Q38.4 What's a typical value for a plasmon-energy loss?
Q38.5 What are inter- and intraband transitions and why do they result in relatively low energy losses?
Q38.6 Why is it important for the ZLP to be the most intense peak in the spectrum by a factor of 10 or more?
Q38.7 What's another expression for the 'permittivity of free space'?
Q38.8 What is meant by the 'free-electron density' and what role does it play in low-energy losses?
Q38.9 Why is the plasmon peak the most prominent energy-loss peak in the spectrum from a thin specimen?

Q38.10 What is the difference between the characteristic and the cut-off angle? Which is more important in EELS and why?
Q38.11 What electrons are in the ZLP?
Q38.12 Under what conditions would you wish to remove the tail of the ZLP?
Q38.13 Describe one other way to measure the dielectric constant apart from low-loss EELS. What are the relative advantages and disadvantages of the two approaches?
Q38.14 What's the best way to remove the tail of the ZLP?
Q38.15 What is fingerprinting and why should you be cautious about using it?
Q38.16 Why would you ever bother to form an image from which the energy-loss electron have NOT been removed?
Q38.17 Why would you ever bother to form a CBED pattern from which the energy-loss electrons have NOT been removed?
Q38.18 What is a Kramers-Kronig transformation? What information does it extract from the low-loss spectrum?
Q38.19 Why hasn't there been more use of plasmon-shift measurements for composition determination?
Q38.20 Explain why you might want to model the intensity in the low-loss spectrum.
Q38.21 Distinguish single, plural, and multiple scattering. Which is best for EELS and why?

TEXT-SPECIFIC QUESTIONS

T38.1 Distinguish the characteristic scattering angle, the cut-off angle, and the spectrometer collection angle. Explain why large differences in the characteristic scattering angle affect the information in the spectrum.
T38.2 Why does filtering out the energy-loss electrons improve the quality of images of specimens showing mass-thickness contrast?
T38.3 Why does filtering out the energy-loss electrons improve the quality of images of specimens showing diffraction contrast?
T38.4 Why does filtering out the energy-loss electrons improve the quality of diffraction patterns?
T38.5 What is contrast tuning and under what circumstance might you use it?
T38.6 Why do you think there's a residual interband transition peak in the polyethylene spectrum in Figure 38.9?
T38.7 Can you think of any other way to image the distribution of Li shown in Figure 38.8 (Hint: read Chapter 39 first)?
T38.8 Why were we able to use plasmon-peak shift measurements as an analysis technique over 30 years ago and why does nobody use it any more?
T38.9 Why does EELS low-loss determination of the dielectric constant compare with UV spectroscopy in terms of the valence states that can be determined? (Hint: work out the wavelength of electrons with a typical low energy loss.)
T38.10 Given that we typically think of the band gap as a non-spatially localized phenomenon due to overlap of the energy states above the atomic potential wells, explain how we can talk about band-gap imaging and the high spatial resolution of images such as Figure 38.10.
T38.11 Why would we want to calculate the intensity distribution in low-loss spectra?
T38.12 Given that the low-loss spectrum is so much more intense than the high-loss spectrum, why has there been relatively little theoretical and experimental work on this part of the spectrum compared with the high-loss regime?
T38.13 Estimate the relative intensities in the zero-loss and the low-loss regions of Figure 38.1 and then explain why we can approximate the total spectrum intensity to the sum of these two components.
T38.14 Study Figure 38.7, then draw diagrams showing how the spectral peaks continue to change in relative intensity with increasing thickness beyond that in Figure 38.7B.
T38.15 Why would you expect to see differences in the low-loss spectra from different compounds such as shown in Figure 38.5?
T38.16 Why do plasmon-like peaks occur in spectra from biological materials in which there are no free electrons?